Molecular Crystals and Liquid Crystals

ISSN: 1542-1406 (Print) 1563-5287 (Online) Journal homepage: http://www.tandfonline.com/loi/gmcl20

Studies on temperature-dependent optical and electro-optical molecular characterization of terephthal-bis 4, n-decylaniline and cholesteryl oleate

T. N. Govindaiah

To cite this article: T. N. Govindaiah (2016) Studies on temperature-dependent optical and electro-optical molecular characterization of terephthal-bis 4, n-decylaniline and cholesteryl oleate, Molecular Crystals and Liquid Crystals, 633:1, 100-109, DOI: 10.1080/15421406.2016.1177890

To link to this article: http://dx.doi.org/10.1080/15421406.2016.1177890

Published online: 24 Aug 2016.

MOLECULAR CRYSTALS AND LIQUID CRYSTALS
2016, VOL. 633, 100–109
http://dx.doi.org/10.1080/15421406.2016.1177890

Taylor & Francis
Taylor & Francis Group

Studies on temperature-dependent optical and electro-optical molecular characterization of terephthal-bis 4, *n*-decylaniline and cholesteryl oleate

T. N. Govindaiah

Research-Center and Post-Graduate Department of Physics, Government College (Autonomous), Mandya, India

ABSTRACT

A binary system of terephthal-bis 4, n-decylaniline (TBDA) and cholesteryl oleate (CO) exhibits a twisted grain boundary (TGB) and induced smectic phases at different concentrations and at different temperatures. Mixtures with higher concentrations of TBDA exhibit I-N*-TGB-SmC-SmA-SmB phases sequentially when the specimen is cooled from its isotropic melt. The temperature variation of optical anisotropy has been discussed. Electro-optical and X-ray studies have also been discussed.

KEYWORDS

Electro-optical studies; molecular orientation; optical anisotropy; temperature dependence

Introduction

Organic materials have been increasingly examined over the past three decades due to their potential applications and interesting properties. Specially, liquid crystals, it is fourth states of matter, are used for different electro-optic devices. Liquid crystal display technology plays a key role at the notebook, computer displays, and flat TV, because of showing full range of color, lower power consumption, and using lower space [1, 2]. They are also used at different areas such as: electro-optic filters [3], holography [4, 5], digital data storage [6–8], and biosensors [8]. Generally, wide temperature range of the liquid crystalline phase, high optical and dielectric anisotropy, and fast switching time are required for modern liquid crystals industrial applications [10, 11].

In the present study, we have considered the binary system of two compounds, viz., terephthal-bis 4, *n*-decylaniline (TBDA) and cholesteryl oleate (CO). Twisted grain boundary and induced smectic phases were observed using microscopic technique and they have been verified from the results of optical anisotropic techniques. Electro-optical and X-ray studies have been discussed.

Experimental studies

Mixtures of different concentrations of TBDA in CO were prepared and were mixed thoroughly. The mixtures of different concentrations of TBDA in CO were kept in desiccators for a long time. The samples were subjected to several cycles of heating, stirring, and centrifuging

CONTACT T. N. Govindaiah tngovi.phy@gmail.com Research-Center and P.G. Department of Physics, Government College (Autonomous), Mandya 571401, India.
Color versions of one or more of the figures in the article can be found online at www.tandfonline.com/gmcl.

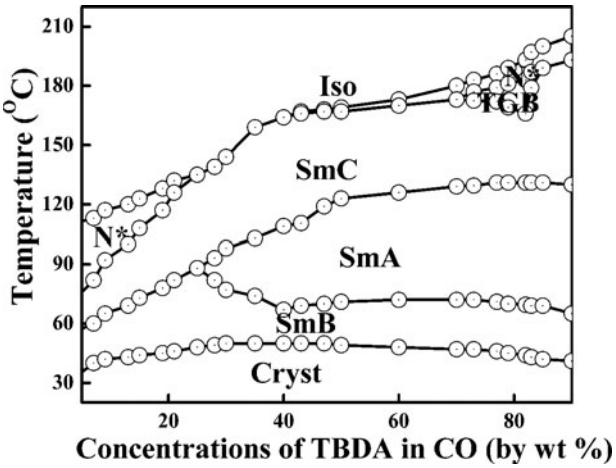

Figure 1. Partial phase diagram for the mixture of TBDA in CO.

to ensure homogeneity. Phase transition temperatures of the mixtures with different concentrations were measured using Leitz-polarizing microscope and conventional hot stage. The sample was sandwiched between the slide and cover slip, which was sealed for microscopic observation. The density and refractive indices of the mixtures were measured at different temperatures employing the technique described in our earlier paper [12]. Electrical conductivity measurements of the given mixture at different temperatures were carried out using digital LCR meter and a proportional temperature control unit. The optical transmittance measurement has been done by placing the cell between two-crossed polarizer's of polarizing microscope model (Radical, RXLr-5) fitted with a hot stage [13]. Electro-optical measurements were carried out by the usual experimental setup of Williams [14]. It consists of tin oxide coated transparent conducting glass plate and the sample sandwiched between these two glass plates. Teflon spacers having thickness of $d = 39 \pm 1$ μm were used and observations were made at 65°C using polarizing microscope in conjunction with a hot stage.

Results and discussions

Phase diagram

The partial phase diagram of given molecules is a very important method to determine the stability of the liquid crystalline phase at different temperatures for different concentrations. The partial phase diagram in the present case is as shown in Fig. 1. This clearly illustrates that the mixtures with concentrations ranging from 70% to 85% of TBDA in CO exhibit Cho (N*), TGB, SmC, SmA and SmB phases sequentially when the specimen is cooled from its isotropic melt. But the mixtures with concentrations ranging from 3% to 25% of TBDA in CO show Cho (N*), SmC and SmB phases, and above 25% shows SmA phase with the other phases at different temperatures [15].

Optical texture studies

When molten sample 79% of TBDA in CO is cooled from its isotropic melt, nucleation starts in the form of minute bubbles and immediately the bubbles grow radially and form fingerprint pattern, which is characteristic of the cholesteric phase with large values of pitch [16, 17]. On further decreasing temperature of the sample, the cholesteric phase changes

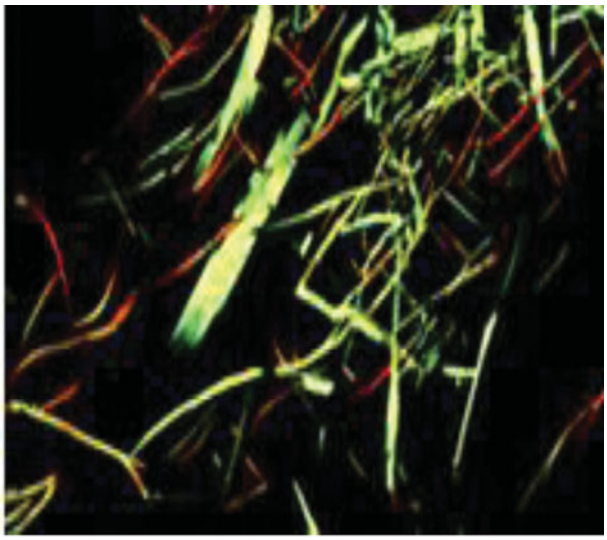

a)

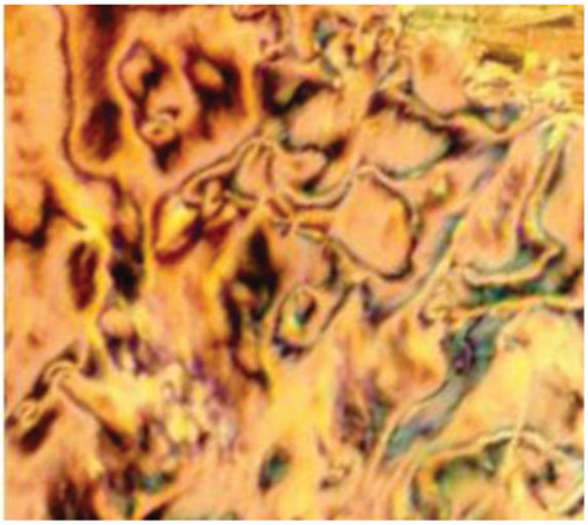

b)

Figure 2. Microphotographs obtained in between the crossed polars: (a) streak-like texture of TGB phase and (b) Schlieren texture of the SmC phase.

over to the smectic phase, passing through an intermediate phase and it is assigned by the appearance of streak-like texture in the form of the homeotropic region, which is the characteristic of the twisted grain boundary phase as shown in Fig. 2(a). The helical axes of the twisted grain boundary phase lie in a direction parallel to the smectic layer planes [18]. On further cooling the specimen, the TGB phase slowly transform to schlieren texture of SmC, which is shown in Fig. 2(b). The molecular structure of the SmC phase is not stable and then it slowly changes over to focal conic fan-shaped texture of the smectic-A phase. Sequentially on cooling specimen, the molecular structure of the SmA phase changes over to the SmB phase and then it becomes the crystalline phase, which remains stable at room temperature [19].

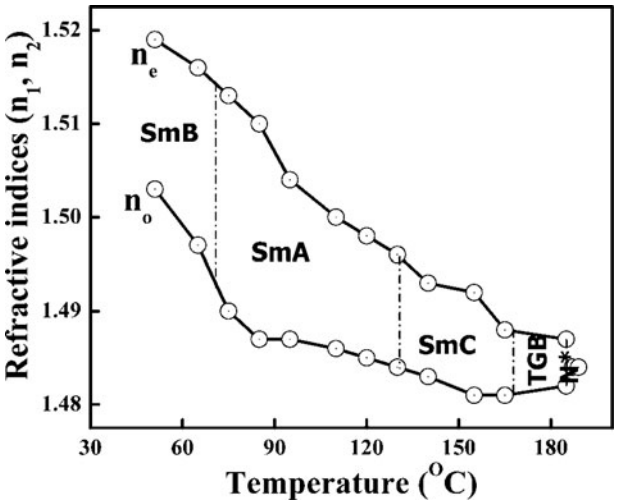

Figure 3. Temperature variations of refractive indices for the mixture of 79% of TBDA in CO.

Optical anisotropy

Results of this investigation have been further complemented by the optical studies. The refractive indices for extraordinary ray (n_e) and ordinary ray (n_o) of the mixture were measured at different temperatures for the different concentrations using Abbe Refractometer. The variations of refractive indices as a function of temperature for 79% of TBDA in CO are shown in Fig. 3. The value of n_e is greater than n_o, indicating that the material is uniaxial positive. The values of electrical susceptibility for 79% of TBDA in CO have been calculated using Neugebauer relation [20] at different temperatures. The variation of electrical susceptibility as a function of temperature for the mixture is shown in Fig. 4. From the figure, it can be observed that wherever there is an isotropic–liquid crystalline phase transition, the value of electrical susceptibility changes appreciably, which indicates that the changes correspond to various smectic modifications. Further, with increase in the concentration of TBDA, the value of electrical susceptibility decreases with temperature because the effective optical anisotropy associated with the molecules of TBDA also decreases.

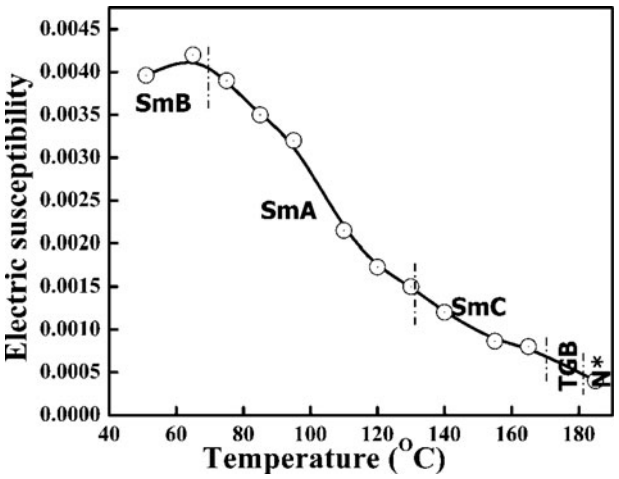

Figure 4. Temperature variation of electrical susceptibility for the mixture of 79% of TBDA in CO.

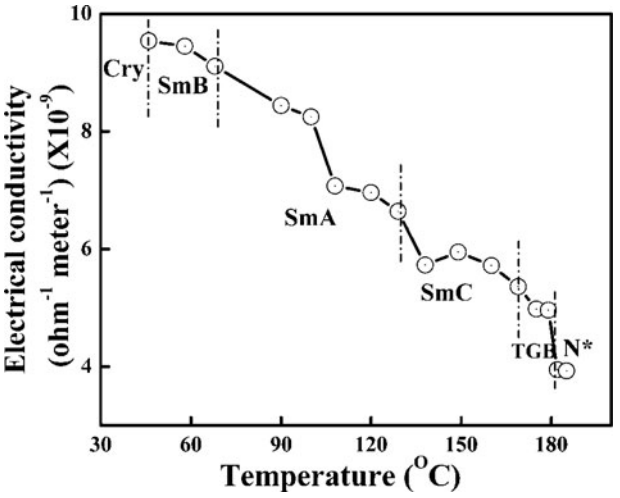

Figure 5. Temperature variation of electrical-conductivity σ ($\times 10^{-9}\ \Omega^{-1}\ m^{-1}$) for the sample of 79% of TBDA in CO.

Conductivity measurements

Phase transition behavior of the liquid crystalline materials with temperature can be very well studied by electrical-conductivity measurements. An abrupt increase or decrease of electrical-conductivity with temperature relates to the phase behavior of the lyotropic and thermotropic systems [21]. The temperature variations of electrical conductivity are shown in Fig. 5, which clearly illustrates that there is some change in the value of electrical conductivity from 45°C to 185°C, while cooling from the isotropic phase for the mixture of 79% of TBDA in CO. The mixture of 79% of TBDA in CO, the sequence of phase changes from N*-TGB-SmC-SmA-SmB phases respectively at different temperatures. Here, it has been found that the electrical conductivity goes on increasing as the temperature decreases. This suggests that aggregated molecular size starts growing toward lower temperatures and then the system becomes more ordered [22, 24, 23–27].

Helical pitch measurements in smectic and cholesteryl layers

The helical pitch measurements were performed on the cholesteric phase in a Grandjean–Cano wedge between a plate and a cylindrical lens treated for homogeneous alignment. The given mixture was cooled slowly from the isotropic phase to the smectic phase, which induced an array of equidistant Grandjean–Cano lines [28, 30]. The pitch of cholesteric (N*) phase was determined by measuring the distance between the Grandjean–Cano lines as a function of temperature. As the temperature was lowered, the mesophase changes from cholesteric (N*) to the smectic phase and the spacing between the lines are increased, indicating that the pitch in the cholesteric (N*) phase is also increasing. The temperature variation of pitch for mixture of 79% of TBDA in CO is shown in Fig. 6. From this figure, it is evident that the variation of pitch from cholesteric (N*) to the smectic phase is smooth and continuous. But gradually, the value of pitch increases from 0.172 to 0.19 mm upon cooling the sample from cholesteric (N*) to the smectic phase. The value of the pitch increases steeply and reaches a maximum of 0.54 mm at the cholesteric (N*) to the smectic phase transition. In this study, we have noticed that the sequence is Iso-N*-TGB-SmC-SmA-SmB on cooling. The pitch is continuous at the cho (N*)–smectic transition in spite of a rather energetic transition [29–33]. It increases on

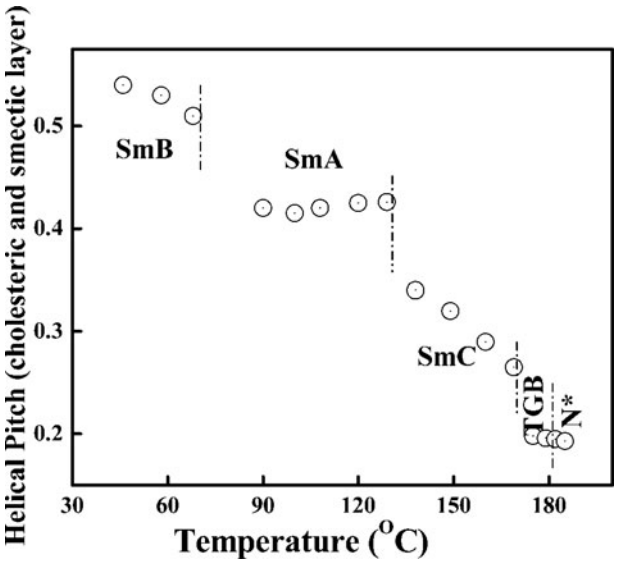

Figure 6. The temperature variations of pitch for the mixture of 79% of TBDA in CO.

cooling to the smectic phase and diverges on approaching the SmC, SmA, and SmB phases. This divergence is related to the second-order transition. It exhibits a steep decrease, close to cholesteric (N*) phase which is usually the characteristics of second-order SmC, SmA, and SmB phase transitions.

Optical transmittance studies

The temperature variation of optical transmittance for mixture of 79% TBDA in CO is presented in Fig. 7. This clearly illustrates that the value of optical transmittance increases slowly with increase in temperature from 45°C to 160°C, while the sequence of phase appears from the crystalline phase to nearer isotropic region and hence suddenly in region of nearer

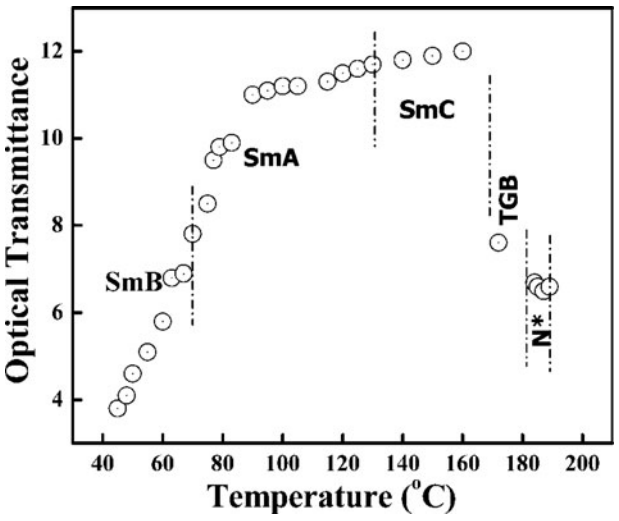

Figure 7. The temperature variation of optical transmittance for the mixture of 79% of TBDA in CO.

isotropic phase some changes have been observed in the value of optical transmittance between the temperature range 172–189°C [34].

The optical transmittance is so continuous toward at SmC-TGB and also at TGB-N* transitions. Here, it can be remarkably noted that the structural molecular orientation of this region is not energetic and it means that it has been decreasing while increasing the temperature and hence it diverges on approaching TGB and N* phases. The divergence of optical transmittance can be related to become a first-order or second-order transition. Here in the present study: the optical transmittance shows a steep decrease and it is very close to the isotropic phase which are the characteristics of first-order transition of N* and TGB phases respectively at different temperatures.

Electro-optical studies

Electro-optical measurements are very important tool in getting better idea on the phase transition behavior of liquid crystalline phases with electric field at constant temperature. In this study, we have been considered the sample for mixture of 79% TBDA in CO at constant temperature 65°C. When the applied voltage increases: the structural molecular arrangements of liquid crystalline phases start to fluctuate and begin to grow and hence it deforms gradually the original position of the structural formations. Remarkably, it has been observed that, if at constant temperature, various aspects of low-frequency effects on given mixture clearly show different directions of molecular orientations/re-orientations and hence it forms a flow patterns: such as stripped pattern and chevron textures. The formations of zig-zag and herringbone patterns are characteristic of chevron textures and also the forming time of these patterns depends on an applied electric field. If there we have been observed a significant difference of electro-mechanical responses of these textures and the stripes of these textures do not have a linear electro-mechanical effect at low fields and at higher fields it shows mechanical vibration. This indicates that the spontaneous polarization has rotated and is no longer parallel to the electric fields. In contrast to the director: the molecular orientations/re-orientations of the layer structures are unchanged by the application of the applied electric field. Sequentially, if we have to increase the applied field above 22.20 V and hence the microscopically observed structural pattern becomes dynamic scattering mode-like and also it has been appearing like an irregularity of molecular orientation/re-orientations of the frustrated liquid crystalline phase. The frustrated liquid crystalline phase arises in that regions, which are probably due to the structural molecular orientations/ re-orientations are not being confirmed in the *X*, *Z*-plane. When the applied field is kept at constant: microscopically we have observed a completely stationary and regular arrangement of two-dimensional hexagonal grid pattern texture and these hexagonal grid pattern textures are presented in Fig. 8. The hexagonal grid pattern textures are gradually deforms with increasing frequency and hence at some stage, it becomes indistinguishable from the chevron texture. However, the hexagonal grid pattern is rather stationary and is formed in a short time at 250 Hz, 23 V. From this figure, it follows that: an extremely regular arrangement of two-dimensional hexagonal grid pattern texture is formed by the applied field. One of the regions is that: the formation of hexagonal grid pattern texture is the electronic charge injected by the applying external electric field [35–38].

Characterization of nano-aggregated grains

The X-ray diffractometer traces obtained for the mixture of 75% and 79% TBDA in CO at temperature 70°C are shown in Fig. 9. The diffraction peaks at these temperatures correspond

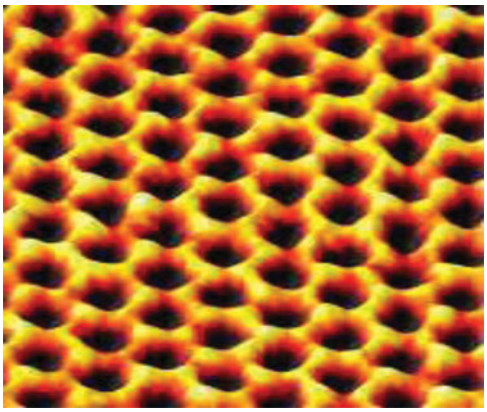

Figure 8. Hexagonal grid pattern electro-optical texture.

to the SmA phase respectively by using JEOL diffractometer with the settings: TC4, CPS400, channel width 100 for $\lambda = 1.934$ Å). X-ray diffraction study is an important method to determine the nano-aggregated grain size of the molecules for different liquid crystalline phases [39, 40]. The deviation from perfect liquid crystallinity leads to broadening of the diffraction peaks. A broad peak in the 2θ range of 4^0-7^0 and has been observed for the given mixtures of different concentrations. However in the given mixtures of additive molecules, the diffraction peak has been found to increase in broadness and decrease in intensity of the peak reveals the increase in the amorphous nature of the additive molecules. In addition to this, the given mixtures of different concentrations can also exhibit a sharp peak, which has been observed in the range 15.5^0-17^0. In order to estimate nano-aggregated grain size of the molecules for different liquid crystalline phases corresponding to broadening of X-ray diffraction peaks, we

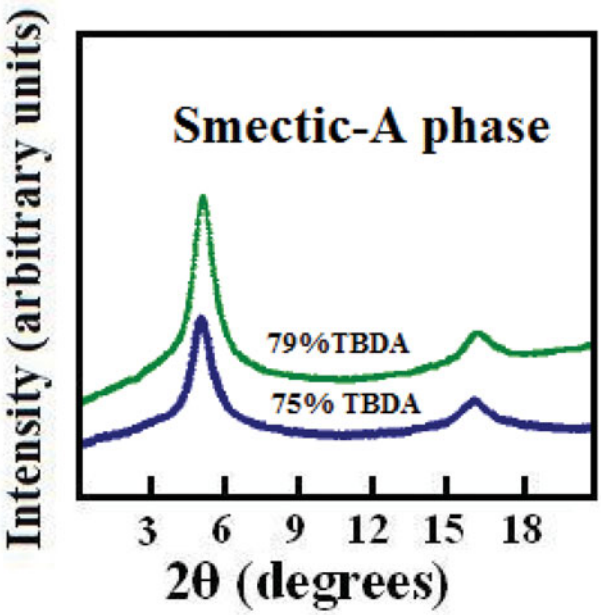

Figure 9. XRD traces obtained for the mixture of 75% and 79% TBDA in CO.

have used the Scherrer's formula

$$L = K\lambda/\beta\cos\theta,$$

where L is the nano-aggregated grain size, λ is the wavelength of X-ray radiation (Fe: 1.934 Å), K is usually taken as 0.89, β is the line width at half maximum, and θ is the diffraction angle. Usually with decrease of temperature [41, 42], the nano-aggregated grain size of the molecules increases. Temperature-dependent molecular orientations of focal conic fan texture of the SmA phase are more stable and hence the molecular ordering of this phase shows two peaks. The nano-aggregated grain size of liquid crystalline material for the SmA phase comes out to be 32.69 nm and 38.28 nm. From the calculated value of nano-aggregated grain size obtained for the given mixtures decreases for the 75% concentration, but it increases above 75% of TBDA. This is because the calculated nano-aggregated grain size is an average value obtained due to all the reflections and hence, the nano-aggregated grain size of the TBDA decreases for lower concentrations, but eventually as the concentration of additive molecule decreases, these values get stabilized and show an increase in nano-aggregated grain size with the increase in concentrations of TBDA. X-ray studies clearly illustrate that the nano-aggregated grain sizes are big enough to indicate that the molecular ordering [43–45] of the layer structure increases as well as decrease in temperature.

Conclusions

In this study, we have observed the existence of TGB and induced smectic phases sequentially, while the sample was cooling from its isotropic melt. The drastic changes in the values of optical anisotropy with temperature unambiguously correspond to different liquid crystalline phases respectively at different temperatures. The experimentally measured optical transmittance has been discussed. Changes in value of the applied field at constant temperature unambiguously correspond to optical purity of the liquid crystalline phases and also the electro-optical effects come into existence with variation on the molecular orientations; the electric field changes the anisotropy and leads to important effects on the processing of the optical materials. X-ray studies are very useful to estimate the grain size of the given molecules at different concentrations of the SmA phase respectively at temperature 70°C.

References

[1] Lee, W., Gau, J. S., & Chen, H. Y. (2005). *Appl. Phys. B.*, (81), 171.
[2] Govindaiah, T. N., & Sreepad, H. R. (2015). *Mol. Liq. J.*, *202*, 75–78.
[3] Wu, S. T. (1989). *Appl. Opt.*, *28*, 48.
[4] Chen, A. G., & Brady, D. J. (1992). *Opt. Lett.*, *17*, 441.
[5] Eich, M., Wendor, J. H., & Makromol. (1987). *Chem. Rapid. Commun.*, *8*, 467.
[6] Khoo, I. C., et al. (1999). *Proc. IEEE.*, *87*, 1897.
[7] Eich, M., Wendor, J. H., Reck, B., Ringsdorf, H., & Makromol. (1987). *Chem. Rapid. Commun.*, *8*, 59.
[8] Matharu, A. S., Jeeva, S., & Ramanujam, P. S. (2007). *Chem. Soc. Rev.*, *36*, 1868.
[9] Woltman, S. J., Jay, G. D., & Crawford, G. P. (2007). *Nature: Mater.*, *6*, 929.
[10] Ozgan, S., & Okumu, M. (2011). *Braz. J. Phys.*, *41*, 118.
[11] Dolgov, L., Yaroshchuk, O., & Lebovka, M. (2008). *Mol. Cryst. Liq. Cryst.*, *496*, 212.
[12] Vardanyan, K. K., Palazzo, E. D., & Walton, R. D. (2011). *Liq. Cryst.*, *38*, 709.
[13] Nagappa, Nataraju, S. K., & Krishanamurti, D. (1986). *Mol. Cryst. Liq. Cryst.*, *133*, 31.
[14] Misra, A. K. (2009). Ph.D., Thesis, University of Lucknow, India.
[15] Williams, R. (1963). *Nature.*, *199*, 273–274.

[16] Govindaiah, T. N., Sreepad, H. R., & Nagappa. (2013). *Mol. Cryst. Liq. Cryst.*, *574*, 9–18.
[17] Govindaiah, T. N., Sreepad, H. R., & Nagappa. (2013). *Mol. Cryst. Liq. Cryst.*, *574*, 1–8.
[18] Govindaiah, T. N., & Sreepad, H. R. (2015). *Phase Trans.*, *88*(4), 368–374.
[19] Nagappa, Revanasiddaiah, D., & Krishnamurti, D. (1983). *Mol. Cryst. Liq. Cryst.*, *101*, 103–127.
[20] Govindaiah, T. N. (2015). *Mol. Cryst. Liq. Cryst.*, *623*, 74–79.
[21] Neugebauer, H. E. J. (1954). *Can. J. Phys.*, *32*(1), 1–8.
[22] Govindaiah, T. N., Sreepad, H.R., & Nagappa. (2015). *Mol. Cryst. Liq. Cryst.*, *609*, 61–69.
[23] Marthandappa, M., Nagappa, & Lokhanatha Rai, K. M. (1991). *J. Phys. Chem.*, *95*, 6369–6372.
[24] Methemitis, C., Morcellet, M., Sabbadin, J., & Francois, J. (1986). *Euro. Poly. J.*, *22*, 619–624.
[25] Govindaiah, T. N., Sreepad, H. R., Sathyanarayana, P. M., Mahadeva, J., & Nagappa. (2012). *Mol. Cryst. Liq. Cryst.*, *552*, 24–32.
[26] Pandey, M. B., Dhar, R., Achalkumar, A. S., & Yelamaggad, C. V. (2007). *J. Phys.: Condens. Matter.*, *19*, 436219.
[27] Goncharuk, A. I., Lebovka, N. I., Lisetski, L. N., & Minenko, S. S. (2009). *J. Phys. D: Applied Phys.*, *42*(16), 165411.
[28] Lisunova, M. O., Mamunya, Y. P., Lebovka, N. I., & Melezhyk, A. V. (2007). *Eur. Polym. J.*, *43*, 949–958.
[29] Ponevchinsky, V. V., et al. (2013). *Proc. SPIE.*, 8637. doi:10.1117/12.2000064.
[30] Govindaiah, T. N., & Sreepad, H. R. (2015). *Phase Trans.*, *88*(4), 368–374.
[31] Govindaiah, T. N., Sreepad, H. R., & Nagappa. (2013). *Mol. Cryst. Liq. Cryst.*, *575*, 22–29.
[32] Balasubramanian, D. (2005). *Photochem. and Photobio.*, *81*, 498–501.
[33] Brunet-Germain, M. (1972).D.Sc. Thesis, University of Sciences and Techniques of Languedoc, Montpellier; see also Brunet-Germain, M. (1972). *C. R. Acad. Sci. (Paris), B.*, *274*, 1036.
[34] Zink, H., & Belyakov, V. A. (1995). *Mol. Cryst. Liq. Cryst.*, *265*, 445.
[35] Belyakov, V. A., & Kats, E. I. (2000). *JETP.*, *91*, 488.
[36] Belyakov, V. A., Oswald, P., & Kats, E. I. (2003). *JETP.*, *96*, 915.
[37] Vaz, N. A., & Montgomery, G. P. (1987). *J. Appl. Phys.*, *62*, 3161.
[38] Helfrich, W. (1973). *Mol. Cryst. Liq. Cryst.*, *21*, 193.
[39] Krishnamurti, D., & Revannasiddaiah, D. (1979). *Mol. Cryst. Liq. Cryst.*, *55*(1), 33–46.
[40] Kai, S., Yamaguchi, K., & Hirakawa, K. (1975). *Japan J. Appl. Phys.*, *14*, 1385.
[41] Hui-Yu, Chen. (2005). *Opt. Rev.*, *12*(3), 223–225.
[42] Sreepad, H. R., & Nagappa. (2015). *Mol. Cryst. Liq. Cryst.*, *609*, 46–53.
[43] Theim, J., Vill, V., & Fischer, F. (1989). *Mol. Cryst. Liq. Cryst.*, *170*, 43–51.
[44] Kumar, V., Joseph, B., Ramteke, P. W., Mani, A., & Jahan, F. (2011). *J. Chem. Pharm. Res.*, *3*(2), 226–233.
[45] Crosa, M., Boero, V., & Franchini-Angela, M. (1999). *Clays and Clay Minerals*, *47*(6), 742–747.